



HAL
open science

Variational Bayesian inversion for microwave imaging applied to breast cancer detection

Leila Gharsalli, H Ayasso, Bernard Duchêne, Ali Mohammad-Djafari

► **To cite this version:**

Leila Gharsalli, H Ayasso, Bernard Duchêne, Ali Mohammad-Djafari. Variational Bayesian inversion for microwave imaging applied to breast cancer detection. ICIPE 2014 - 8th International Conference on Inverse Problems in Engineering (ICIPE 2014), May 2014, Cracovie, Poland. pp.ID 5-2. hal-01103636

HAL Id: hal-01103636

<https://centralesupelec.hal.science/hal-01103636>

Submitted on 27 May 2015

HAL is a multi-disciplinary open access archive for the deposit and dissemination of scientific research documents, whether they are published or not. The documents may come from teaching and research institutions in France or abroad, or from public or private research centers.

L'archive ouverte pluridisciplinaire **HAL**, est destinée au dépôt et à la diffusion de documents scientifiques de niveau recherche, publiés ou non, émanant des établissements d'enseignement et de recherche français ou étrangers, des laboratoires publics ou privés.

Variational Bayesian inversion for microwave imaging applied to breast cancer detection

L. Gharsalli¹, H. Ayasso², B. Duchêne¹, A. Mohammad-Djafari¹

¹ Laboratoire des Signaux et Systèmes (L2S), (UMR8506: CNRS-SUPELEC-Univ Paris-Sud),
3 rue Joliot-Curie, 91190 Gif-sur-Yvette, France

² GIPSA-LAB, Département Image Signal, (CNRS-Univ Grenoble),
BP 46 - 38402, Saint Martin d'Hères, France
e-mail: leila.gharsalli@lss.supelec.fr

Key words: Inverse scattering, microwave imaging, breast cancer detection, Gauss-Markov-Potts prior, Variational Bayesian Approximation

Abstract

In this work, microwave imaging is considered as a nonlinear inverse scattering problem and tackled within a Bayesian estimation framework. The object under test (breast affected by a tumor) is supposed to be composed of compact regions made of a restricted number of different homogeneous materials. This *a priori* knowledge is appropriately translated by a Gauss-Markov-Potts prior. First, we express the *a posteriori* probability laws of all the unknowns and then the Variational Bayesian Approximation (VBA) used to compute the posterior estimators and reconstruct both permittivity and conductivity maps. This approximation consists in the best separable probability law that approximates the true posterior probability law in the Kullback-Leibler sense. This leads to an implicit parametric optimization scheme which is solved iteratively. Some preliminary results, obtained by applying the proposed method to synthetic data, are presented and compared to those obtained by means of the classical contrast source inversion method.

1 Introduction

In the last few decades, microwave scattered imaging has received an increasing interest for medical applications such as breast cancer detection [1]. In addition to the non-ionizing nature of microwaves, one of the motivation for developing a microwave imaging technique for detecting breast cancer is the significant contrast that exists at microwave frequencies between the dielectric properties of normal and malignant breast tissues. All this makes microwave imaging a better alternative, in terms of cost and harmlessness, than X-ray mammography which is the most current breast cancer detection technique.

Hence, measurements of the scattered fields resulting from the interaction between a known interrogating wave in the microwave frequency range and the breast can be used to retrieve a contrast function representative of the dielectric properties (permittivity and conductivity) of the latter. This leads to a non linear ill-posed inverse scattering problem solved, herein, in a variational Bayesian framework. The associated forward problem consists in modeling the wave-breast interaction through a domain integral representation of the electric field in a 2-D configuration in a transverse magnetic polarization case.

The Bayesian framework allows us to take easily into account *a priori* information on the sought solution. Herein, we would like to account for the fact that the breast is composed of a finite number of different tissues distributed in compact regions, meaning that the sought image is composed of a finite number of homogeneous area. This *a priori* is introduced via a Gauss-Markov fields with hidden Potts label fields [2]. Afterwards, the variational Bayesian approximation (VBA) [3] is applied to obtain an estimator of the posterior law. It can be noted that a semi-supervised context is considered herein where the number of different tissues is supposed to be known, while all the unknowns and hyper-parameters of the model are estimated simultaneously through a joint posterior law. The purpose of VBA is to approximate the latter by a free form distribution that minimizes the Kullback-Leibler divergence. This distribution is chosen as a separable law. Then, thanks to the latter method, the initial inverse problem turns into an optimization problem and an analytical approximation of the posterior is obtained. Its use in microwave imaging and optical diffraction tomography has already been treated and results have shown its performances with respect to the computation time and simplicity, compared to other methods such as Monte-Carlo Markov Chain (MCMC) [4, 5].

The main contribution of this work is the application of VBA to breast imaging where the sought contrast is complex valued, contrarily to the case treated in [5], and both permittivity and conductivity maps have to be retrieved. Herein, we discuss the results obtained by means of this approach from synthetic data generated in different configurations involving two different numerical breast phantoms: a simple model made of two homogeneous media and a more sophisticated one built up from a MRI scan of a real breast. Then we present results compared to those obtained by means of the deterministic contrast source inversion method (CSI, [13]).

The paper is organized as follows: section 2 is about the experimental configuration and the forward modeling. The VBA approach and Bayesian computations are discussed in section 3. In section 4, the method is applied to synthetic data and is compared to CSI. Finally, some conclusions and perspectives are given in section 5.

2 The forward modelling

2.1 The experimental configuration

We consider a 2-D configuration in a transverse magnetic polarization case where the object under test is supposed to be cylindrical, of infinite extension along the z axis and illuminated by a line source whose location can be varied and that operates at several discrete frequencies. This source generates an incident electric field E^{inc} polarized along the z axis with an $\exp(-i\omega t)$ implicit time dependence and illuminates the breast from 64 various angular positions uniformly distributed around a 7.5-cm-radius circle centered at the origin and at 6 different frequencies in the band 0.5 - 3 GHz. For each frequency and illumination angle, 64 measurements of the scattered field are performed at angular positions uniformly distributed around the same circle. The breast (domain \mathcal{D}_2) is immersed in a background medium (domain \mathcal{D}_1) and is

supposed to be contained in a test domain (\mathcal{D}). The different media are characterized by their propagation constant $k(\mathbf{r})$ such that $k(\mathbf{r})^2 = \omega^2 \epsilon_0 \epsilon_r(\mathbf{r}) \mu_0 + i\omega \mu_0 \sigma(\mathbf{r})$, where ω is the angular frequency, ϵ_0 and μ_0 are the permittivity and the permeability of free space, respectively, $\mathbf{r} \in \mathcal{D}$ is an observation point and $\epsilon_r(\mathbf{r})$ and $\sigma(\mathbf{r})$ are the relative permittivity and conductivity of the medium.

Two models of breast are considered herein (Figure 1). Both of them are supposed to be affected by a tumor (domain \mathcal{D}_3) with a 2-cm-diameter circular cross-section and of electromagnetic parameters $\epsilon_r = 55.3$ and $\sigma = 1.57 \text{ Sm}^{-1}$. The first model (Model-1) is rather simple: it consists in an homogeneous breast, with a 9.6-cm-diameter circular cross-section and relative dielectric permittivity and conductivity respectively equal to $\epsilon_r = 6.12$ and $\sigma = 0.11 \text{ Sm}^{-1}$, immersed in a background medium of electromagnetic parameters $\epsilon_r = 10$ and $\sigma = 0.5 \text{ Sm}^{-1}$. The second model (Model-2) is more sophisticated. It is built up from a MRI scan of a real breast. Hence, the breast is also supposed to be of circular cross-section with a diameter of 9.2 cm but it is now made of a very heterogeneous medium with parameters varying in the ranges $2.46 \leq \epsilon_r \leq 60.6$ and $0.01 \text{ Sm}^{-1} \leq \sigma \leq 2.28 \text{ Sm}^{-1}$, surrounded by a skin with electromagnetic parameters $\epsilon_r = 35.7$ and $\sigma = 0.32 \text{ Sm}^{-1}$ and immersed in a background medium whose relative dielectric permittivity and conductivity are respectively equal to $\epsilon_r = 35$ and $\sigma = 0.5 \text{ Sm}^{-1}$.

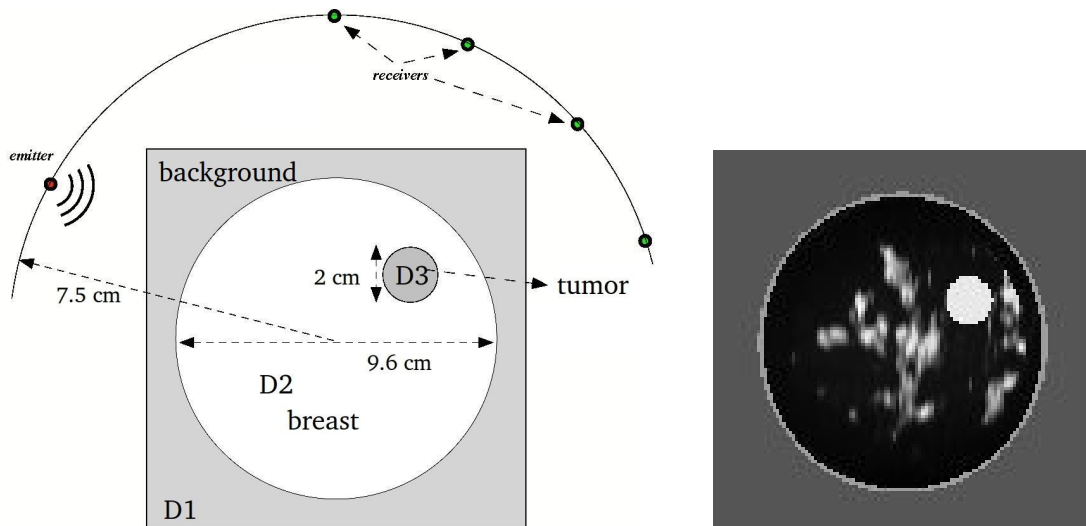


Figure 1: The measurement configuration and the two models of breast (left: Model-1, right: Model-2).

2.2 The problem formulation

The modeling is based upon domain integral representations obtained by applying Green's theorem to the Helmholtz wave equations satisfied by the fields and by accounting for continuity and radiation conditions [8]. The forward model is described by two coupled integral equations. The first one, denoted as the observation equation, is a Fredholm first kind integral equation that relates the scattered field to Huygens-type sources induced within the target by the incident wave, whereas the second one, denoted as the coupling (or state) equation, relates the total field to the induced sources [9, 4]. The forward problem is solved from discrete counterparts of these integral equations obtained by means of a method of moments which pulse basis and point matching [10], which results in partitioning the test domain \mathcal{D} into $N_{\mathcal{D}}$ elementary pixels small enough to permit considering both the field and the contrast as constant

over each of them. Let us now consider a contrast function χ , defined in \mathcal{D} and null outside the object, such that $\chi(\mathbf{r}) = (k(\mathbf{r})^2 - k_1^2)/k_1^2$, where k_1 is the propagation constant of the background medium, and define the Huygens-type sources $w(\mathbf{r})$ as $w(\mathbf{r}) = \chi(\mathbf{r})E(\mathbf{r})$, where $E(\mathbf{r})$ is the total field in the target. The above-mentioned discrete counterparts then read:

$$\mathbf{y} = \mathbf{G}^o \mathbf{w} + \boldsymbol{\epsilon} \quad (1)$$

$$\mathbf{w} = \mathbf{X} \mathbf{E}^{inc} + \mathbf{X} \mathbf{G}^c \mathbf{w} + \boldsymbol{\xi}, \quad (2)$$

where $\mathbf{X} = \text{diag}(\chi)$, \mathbf{E} , χ and \mathbf{w} are vectors that contain the values of $E(\mathbf{r}')$, $\chi(\mathbf{r}')$ and $w(\mathbf{r}')$ at the centers \mathbf{r}' of the pixels ($\mathbf{r}' \in \mathcal{D}$), \mathbf{y} is the vector containing the values of the scattered field $y(\mathbf{r})$ at the measurement points \mathbf{r} , \mathbf{G}^o and \mathbf{G}^c are huge matrices whose elements result from the integration of the Green's function over the elementary pixels [5] and $\boldsymbol{\epsilon}$ and $\boldsymbol{\xi}$ are two variables that account for the model and measurement errors and that are supposed to be centered and white and to satisfy Gaussian laws (i.e., $\boldsymbol{\epsilon} \sim \mathcal{N}(\boldsymbol{\epsilon}|\mathbf{0}, v_\epsilon \mathbf{I})$ and $\boldsymbol{\xi} \sim \mathcal{N}(\boldsymbol{\xi}|\mathbf{0}, v_\xi \mathbf{I})$).

Now, the forward problem consists in first solving equation (2) for the induced sources \mathbf{w} , knowing the contrast χ and the incident field \mathbf{E}^{inc} , and then solving equation (1) for the scattered field \mathbf{y} . At this point it can be noted that the synthetic data of the inverse problem are generated in this way. However, in the case of Model-1, in order to avoid committing an inverse crime which would consist in testing the inversion algorithm on data obtained by means of a model closely related to that used in the inversion, the data are computed by benefiting from the circular symmetry that exists in the absence of the tumor. Hence, the data are computed by means of a model (the data model) where only the domain \mathcal{D}_3 occupied by the tumor is discretized, whereas the breast and the background medium are considered as a cylindrically stratified embedding medium and the Green's function is modified consequently. Figure 2 displays the scattered fields obtained by means of the data model on configuration Model-1 for an illumination angle of 45° and at two operating frequencies: 1.5 GHz and 3 GHz, compared to that obtained by means of the forward model used for inversion where the test domain \mathcal{D} is a 12.16 cm sided square partitioned into 64×64 square pixels with side $\delta = 1.9$ mm. It can be observed that the results fit relatively well.

3 Bayesian inversion approach

3.1 Hierarchical prior model

The inverse problem consists in retrieving the unknown contrast χ , or more precisely the relative permittivity ϵ_r and the conductivity σ , from the scattered field \mathbf{y} , given the incident field \mathbf{E}^{inc} . It can be noted that the induced sources \mathbf{w} being also unknown, they must be retrieved at the same time as χ . Hence, assuming that their relation to the contrast is given by the state equation (2), we define their *a priori* probability law as:

$$p(\mathbf{w}|\chi) = \exp \left\{ -\frac{1}{2v_\epsilon} \|\mathbf{w} - \mathbf{X} \mathbf{E}^{inc} - \mathbf{X} \mathbf{G}^c \mathbf{w}\|^2 \right\}. \quad (3)$$

Now, let us introduce *a priori* information on the sought solution required in order to counteract the ill-posedness of the inverse problem. It consists in the fact that the sought object is composed of a restricted number K of homogeneous materials distributed in compact regions. This prior information is introduced by means of a hidden variable (or classification label) $z(\mathbf{r})$ associated with each pixel \mathbf{r} , which represents a segmentation of the unknown object. The finite number of homogeneous materials can then be accounted for through the following conditional distribution:

$$p(\chi(\mathbf{r})|z(\mathbf{r}) = k) = \mathcal{N}(m_k, v_k), \quad k = 1, \dots, K, \quad (4)$$

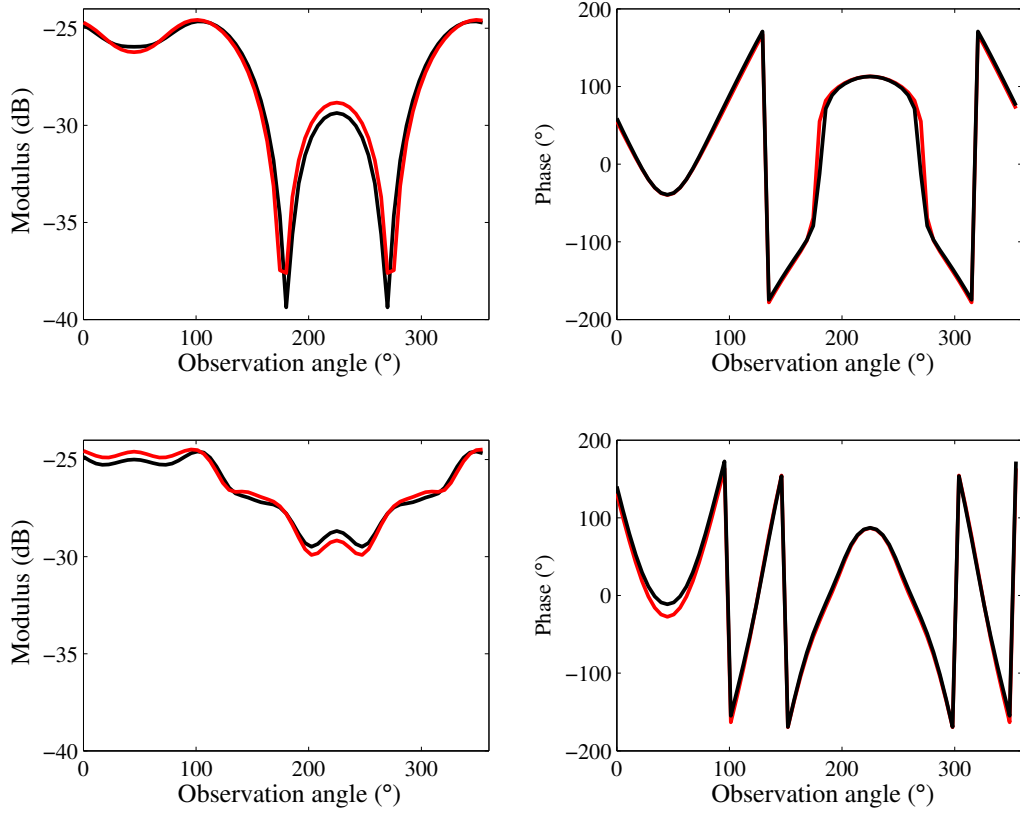


Figure 2: Amplitude (left) and phase (right) of the scattered fields computed by means of the data model (black) and by means of the forward model used for inversion (red) at 1.5 GHz (up) and 3 GHz (down).

which means that all the pixels with the same label ($z(\mathbf{r}) = k$, $k \in \{1, \dots, K\}$) correspond to the same material with a mean value m_k and a variance v_k .

The compactness of the different regions can be accounted for by relating, in a probabilistic way, the classification label $z(\mathbf{r})$ of a pixel \mathbf{r} to that of its neighbors. This is done *via* a Potts-Markov model on z :

$$p(z|\lambda) = \frac{1}{T(\lambda)} \exp \left\{ \lambda \sum_{\mathbf{r} \in \mathcal{D}} \sum_{\mathbf{r}' \in V_{\mathbf{r}}} \delta(z(\mathbf{r}) - z(\mathbf{r}')) \right\}, \quad (5)$$

where λ is a parameter that determines the correlation between neighbors (herein $\lambda = 1$), $T(\lambda)$ is a normalization factor and $V_{\mathbf{r}}$ is a neighborhood of \mathbf{r} , herein made of the four nearest pixels.

Now we have all the components necessary to find the expression of the joint posterior law of all the unknowns $(\boldsymbol{\chi}, \mathbf{w}, \mathbf{z}, \boldsymbol{\psi})$ with $\boldsymbol{\psi} = \{\mathbf{m}, \mathbf{v}, v_\epsilon, v_\xi\}$. The latter is obtained by applying the Bayes formula:

$$\begin{aligned} p(\boldsymbol{\chi}, \mathbf{w}, \mathbf{z}, \boldsymbol{\psi}|\mathbf{y}) &\propto p(\mathbf{y}|\mathbf{w}, v_\epsilon) p(\mathbf{w}|\boldsymbol{\chi}, v_\xi) p(\boldsymbol{\chi}|\mathbf{z}, \mathbf{m}, \mathbf{v}) \\ &\times p(\mathbf{z}|\lambda) p(m_k|\mu_0, \tau_0) p(v_k|\eta_0, \phi_0) \\ &\times p(v_\epsilon|\eta_\epsilon, \phi_\epsilon) p(v_\xi|\eta_\xi, \phi_\xi). \end{aligned} \quad (6)$$

Expressions of $p(\mathbf{y}|\mathbf{w}, v_\epsilon)$, $p(\mathbf{w}|\boldsymbol{\chi}, v_\xi)$ and $p(\mathbf{z}|\lambda)$ are derived respectively from equations (1), (3) and (5), whereas conjugate priors laws are assigned to the hyper-parameters:

$$\begin{aligned} p(m_k) &= \mathcal{N}(m_k|\mu_0, \tau_0), & p(v_k) &= \mathcal{IG}(v_k|\eta_0, \phi_0) \\ p(v_\epsilon) &= \mathcal{IG}(v_\epsilon|\eta_\epsilon, \phi_\epsilon), & p(v_\xi) &= \mathcal{IG}(v_\xi|\eta_\xi, \phi_\xi), \end{aligned} \quad (7)$$

where $\mathcal{N}(m|\mu, \tau)$ and $\mathcal{IG}(v|\eta, \phi)$ stand for Gaussian and inverse-gamma distributions, respectively, and $\mu_0, \tau_0, \eta_0, \phi_0, \eta_\epsilon, \phi_\epsilon, \eta_\xi$ and ϕ_ξ are meta-hyper-parameters appropriately set to have non-informative priors, i.e. flat prior distributions.

3.2 The Variational Bayesian Approach

All the right-hand side expressions of equation (6) are known, which allows us to obtain the left hand side, i.e. the joint posterior law of all the unknowns, up to a normalizing constant. However, the complexity of its expression makes it very hard to obtain in a tractable form for conventional estimators, such as JMAP or PM, and an approximation is then required. Hence, we opt for an analytical approximation based upon the Variational Bayesian Approach (VBA, [11]) which aims in approximating the true posterior distribution (6) by a simpler separable law $q(\mathbf{u}) = \prod_i q(\mathbf{x}_i)$ with $\mathbf{u} = \{\boldsymbol{\chi}, \mathbf{w}, \mathbf{z}, \boldsymbol{\psi}\}$, that minimizes the Kullback-Leibler divergence $\text{KL}(q||p) = \int q \ln(q/p)$. We define the separable law as:

$$q(\mathbf{u}) = q(v_\epsilon)q(v_\xi) \prod_i q(\chi_i)q(w_i)q(z_i) \prod_k q(m_k)q(v_k). \quad (8)$$

Then we look for the optimal form of q that minimizes the Kullback divergence. This leads to the following parametric distributions:

$$\begin{aligned} q(\mathbf{w}) &= \mathcal{N}(\tilde{\mathbf{m}}_w, \tilde{\mathbf{V}}_w), & q(\boldsymbol{\chi}) &= \mathcal{N}(\tilde{\mathbf{m}}_\chi, \tilde{\mathbf{V}}_\chi), & q(\mathbf{z}) &= \prod_r \tilde{\zeta}_k(\mathbf{r}) \\ q(m_k) &= \mathcal{N}(\tilde{\mu}_k, \tilde{\tau}_k), & q(v_k) &= \mathcal{IG}(\tilde{\eta}_k, \tilde{\phi}_k) \\ q(v_\epsilon) &= \mathcal{IG}(\tilde{\eta}_\epsilon, \tilde{\phi}_\epsilon), & q(v_\xi) &= \mathcal{IG}(\tilde{\eta}_\xi, \tilde{\phi}_\xi), \end{aligned} \quad (9)$$

where the tilded variables are mutually dependent and are computed in an iterative way [5].

3.3 Initialization and convergence of the algorithm

The initial number of classes K used for segmentation, it is set to $K = 3$ for Model-1 and $K = 8$ for Model-2, whereas the initial values of the unknowns $\boldsymbol{\chi}^{(0)}$ and $\mathbf{w}^{(0)}$ are obtained by backpropagating the scattered field data from the measurement circle onto the test domain \mathcal{D} . From $\boldsymbol{\chi}^{(0)}$ and $\mathbf{w}^{(0)}$, the classification \mathbf{z} and the hyper-parameters (means and variances) can be initialized by means of *K-means* clustering [12]. Here, given the fact that the contrast is complex valued, first the real part is segmented and, then, the same segmentation is used to initialize the imaginary part. Concerning the convergence, the shaping parameters of the equation (9) are iterated until the convergence is reached. The latter is estimated empirically by looking to the evolution of contrast and hyper-parameters in the course of iterations (figure (3)).

4 Results

Figure (4) displays the results obtained for the conductivity of Model-1 after 500 iterations. These results are compared to those obtained, after the same number of iterations, by means of the contrast source

inversion method (CSI, [7]), an iterative deterministic method which consists in minimizing a cost functional, that accounts for both observation and coupling equations, by alternately updating \mathbf{w} and χ with a gradient-based method. In general, the algorithm succeeds in retrieving homogeneous regions that correspond to the background, the breast and the tumor. The results are, however, more accurate than those

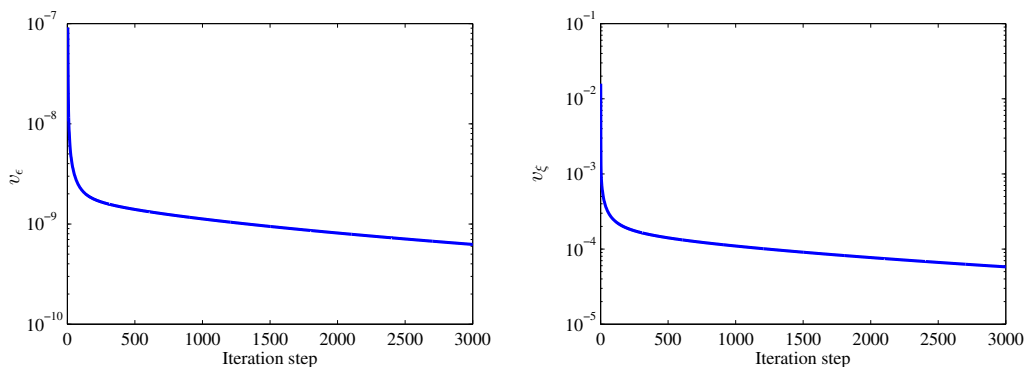


Figure 3: The evolution of the observation v_ϵ (left-) and coupling v_ξ (right) error variances as functions of the iteration step for Model-1.

obtained by means of CSI. This is confirmed by the profiles reconstructed with both methods along an horizontal line crossing the center of the tumor (figure 4 - (d)). Besides, the interest of VBA is that, in addition to an image of the sought object, it yields also an estimate of the hyper-parameters, the segmentation and the variances of the estimators.

Figure (5) displays the results obtained on Model-2, with a test domain \mathcal{D} partitioned into 120×120 1-mm-side square pixels, after 2000 iterations. This figure highlights the observations made on Model-1 about the effectiveness of the proposed VBA technique. The glandular areas in the breast are not exactly found, which is normal as they do not correspond to compact homogeneous regions, but, on the contrary, the tumor is more apparent with VBA than with CSI, particularly in the conductivity map.

5 Conclusion

We consider microwave imaging as an inverse obstacle scattering problem which is known to be ill-posed. This means that a regularization of the problem is required prior to its resolution, and this regularization generally consists in introducing *a priori* information on the sought solution. Herein, an important knowledge about the object under test is that it is composed of a restricted number of homogeneous materials distributed in compact regions. This is tackled in a Bayesian inversion framework via a Gauss-Markov-Potts model. Application to synthetic data shows a good improvement in the reconstruction quality compared to a CSI deterministic approach. However, several points still need to be investigated. Particularly, concerning the convergence fastness, a gradient-like variational Bayesian method [14] is under investigation. This technique has already shown its effectiveness compared to the classical VBA, especially in terms of convergence fastness, in other applications. Furthermore, the use of Gauss-Markov mixtures [4] as prior model for the unknown object may be more adapted, especially when the latter is very heterogeneous, since with this model the links between pixels of the same class are strengthened by means of a Markov field, while the independence between pixels of different classes is kept in order to preserve the contours. An other point is under investigation concerning the number

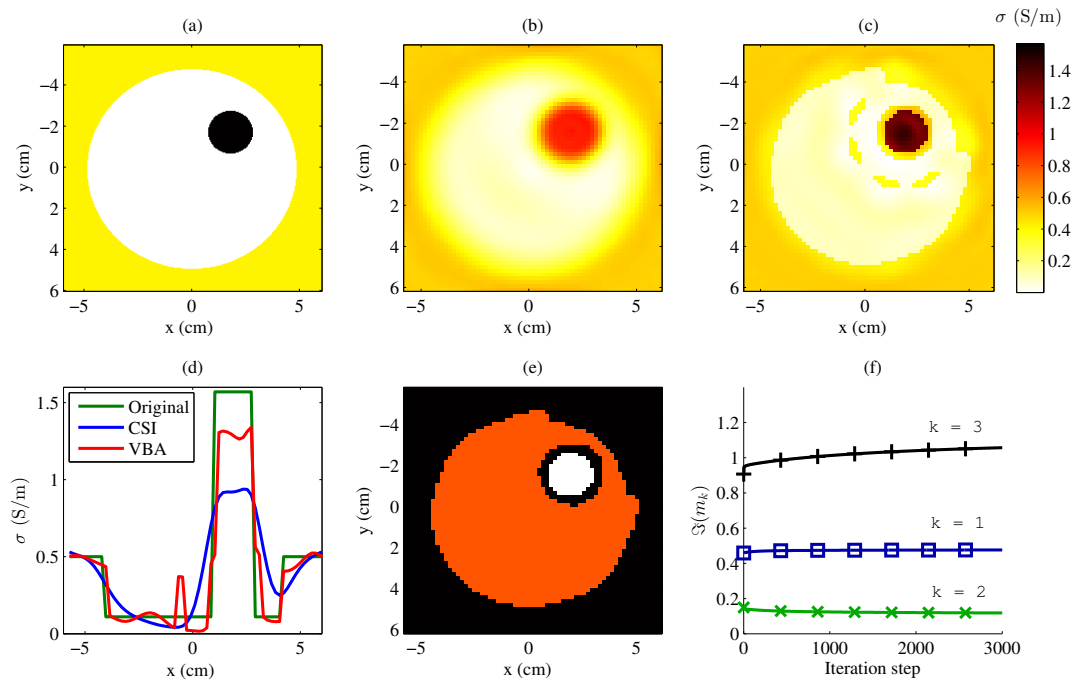


Figure 4: The results obtained for Model-1: maps of conductivity (first row) reconstructed by means of CSI (b) and VBA (c) compared to the real object (a) and (second row) the conductivity profiles reconstructed by means of CSI and VBA compared to the real profile (d), the hidden field (e) and the mean m_k of the imaginary part of the contrast (f) for the 3 classes.

of classes: the latter should converge to an optimal number, if initialized with a higher number, because, during iterations, the number of pixels that belong to some of the classes decreases, which means that the latter should disappear. Alternatively, the estimation of the number of classes, if the latter is unknown, can be tackled by means of a non-parametric approach.

References

- [1] T. Henriksson, *Contribution to quantitative microwave imaging techniques for biomedical applications*, Ph.D. thesis, Université Paris-Sud 11 - Mälardalen University, (2009).
- [2] A. Mohammad-Djafari, *Gauss-Markov-Potts priors for images in computer tomography resulting to joint optimal reconstruction and segmentation*, International Journal of Tomography and Statistics, 11: W09, (2008), pp. 76–92.
- [3] D.J.C. Mackay, *Information Theory, Inference, and Learning Algorithms*, Cambridge University Press, (2003).
- [4] H. Ayasso, *Une approche bayésienne de l'inversion. Application à l'imagerie de diffraction dans les domaines micro-onde et optique*, Ph.D. thesis, Université Paris sud 11, (2010).
- [5] H. Ayasso, B. Duchêne, and A. Mohammad-Djafari, *Optical diffraction tomography within a variational Bayesian framework*, Inverse Problems in Science and Engineering, 20, no. 1, (2012), pp. 59–73.

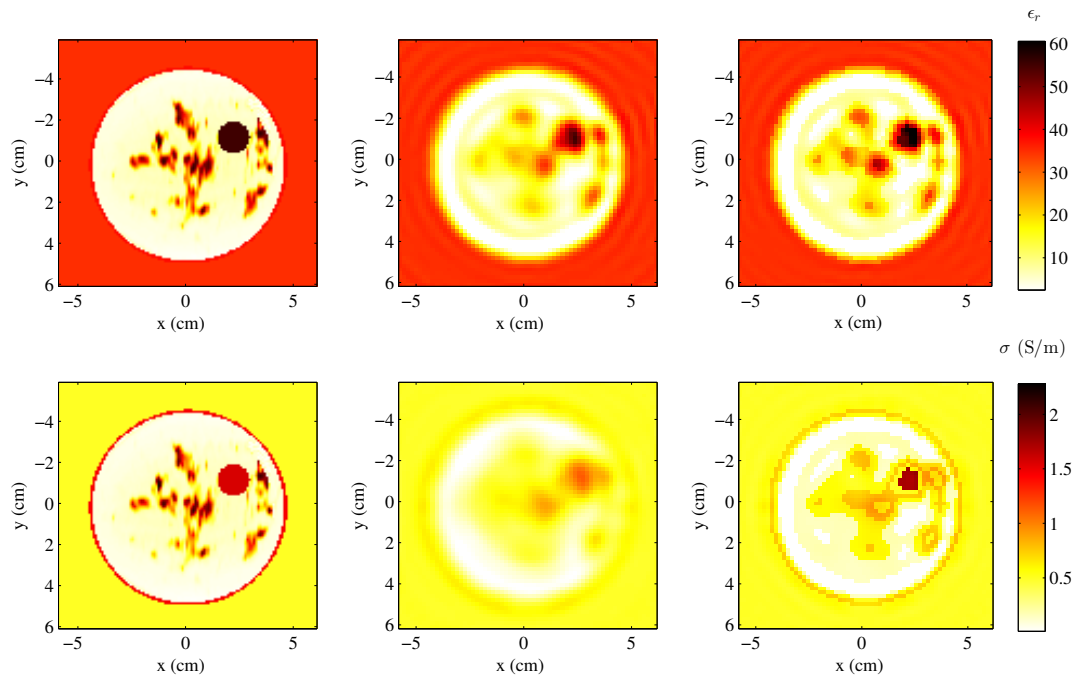


Figure 5: The results obtained for Model-2: maps of permittivity (up) and conductivity (down) reconstructed by means of CSI (second column) and VBA (third column) compared to the real object (first column).

- [6] L. Gharsalli, H. Ayasso, B. Duchêne, and A. Mohammad-Djafari, *Microwave tomography for breast cancer detection within a Variational Bayesian Approach*, IEEE European Signal Processing Conference, EUSIPCO, Marrakech (2013).
- [7] P.M. van den Berg, A. van Broekhoven, and A. Abubakar, *Extended contrast source inversion*, Inverse problems, 15, (1999), pp. 1325–1344.
- [8] W.C. Chew, *Waves and Fields in Inhomogeneous Media*, IEEE Computer Society Press, (1999).
- [9] O. Féron, B. Duchêne, and A. Mohammad-Djafari, *Microwave imaging of inhomogeneous objects made of a finite number of dielectric and conductive materials from experimental data*, Inverse Problems, 21, no. 6, (2005), pp. S95–S115.
- [10] W.C. Gibson, *The Method of Moments in Electromagnetics*, Chapman & Hall/CRC, Boca Raton, (2008).
- [11] V. Smídl, A. Quinn, *The Variational Bayes Method in Signal Processing*, Springer Verlag, Berlin, (2006).
- [12] J.B. MacQueen, *Some Methods for Classification and Analysis of Multivariate Observations*, Univ. California Press, vol. 1, (1967), pp. 281–297.
- [13] P.M. van den Berg, R.E. Kleinman, *A contrast source inversion method*, Inverse Problems, 13, no. 6, (1997), pp. 1607–1620.
- [14] A. Fraysse, T. Rodet, *A gradient-like variational Bayesian algorithm*, Statistical Signal Processing Workshop (SSP), (2011), pp. 605–608.